Mechanical damage characteristics of elementary hemp fibers and scale effect of fiber strength

J. Andersons[1] & R. Joffe[2]
[1]*Institute of Polymer Mechanics, University of Latvia, Rīga, Latvia*
[2]*Division of Polymer Engineering, Luleå University of Technology, Luleå, Sweden*

Abstract

Ecological and economical considerations foster replacement of man-made fibers by natural renewable fibers in various industrial applications. Bast fibers of such plants as, e.g., flax, hemp, jute etc., are particularly attractive as a reinforcement of polymer-matrix composites due to their high specific stiffness and strength in the axial direction. The elementary bast fibers exhibit pronounced scatter of strength. It necessitates probabilistic description of their strength via a distribution function that reflects damage morphology and severity in fibers. Fiber fracture is shown to originate from mechanical defects of the bast cell wall, the most prominent of them being kink bands. While the number of kink bands in a fiber is easily determined by optical microscopy, direct experimental measurement of their strength is complicated. Therefore, alternative approaches are sought, enabling extraction of strength characteristics of the kink bands from fiber tests via appropriate probabilistic models. Analytical distribution function of bast fiber strength has been derived, allowing for the effect of mechanical damage in the form of kink bands. The fiber characteristics measured have been used to evaluate the kink band density and strength distributions. The theoretical distribution is verified against experimental tensile strength data of elementary hemp fibers at several gauge lengths and found to provide acceptable accuracy in predicting the scale effect of strength.
Keywords: hemp, bast fibers, scale effect, Weibull distribution.

WIT Transactions on The Built Environment, Vol 124,
www.witpress.com, ISSN 1743-3509 (on-line)
doi:10.2495/HPSM120141

1 Introduction

The bast fibers of hemp and flax are among the strongest and stiffest plant fibers due to their high content of cellulose fibrils, located in the secondary cell wall taking up most of the fiber cross section, and the relatively low angle of fibril orientation with respect to fiber axis [1]. The remarkable mechanical properties ensured application of bast fibers as reinforcement in polymer matrix, producing composites with reasonable characteristics already in 1930s [2]. Growing ecological concerns have lately renewed interest in natural, sustainably produced fibers. Moreover, lower density of natural fibers than that of man-made ones provides additional competitive advantage in reducing the weight of the composite part [3]. Flax requiring probably the most intensive agro-chemical treatment, hemp may be preferential [4] provided that fiber mechanical properties are not inferior.

Natural fiber properties are highly variable, depending on the variety, growth conditions, retting and pre-processing methods, and even fiber location in the plant stem. Hemp fiber strength is slightly (but statistically significantly) dependent of the time of growth (increasing from 99 to 114 days of growth, then decreasing again) [5]. Although both flax and hemp fibers extracted from the middle part of the stem exhibit higher strength than those from the top and bottom parts, the effect is almost negligible for hemp [6]. Hemp fiber strength is shown to decrease with the increase in fiber diameter (measured near the fracture point), and fibers tend to break within regions where diameter is smaller than the average [6].

Although considerable amount of research has been dedicated to the mechanical properties of hemp fibers [5−17], relatively little attention was paid to the factors determining strength, its scatter, and strength-length scaling of the fibers [5–8, 11]. However, efficient mechanistic models of both fiber fracture process and the reliability of their composites would be instrumental in ensuring wider application of natural fibers in load-bearing, structural composite materials.

Fiber fracture is shown to originate from defects of the bast cell wall [7]. As expected for probabilistic, defect-related fracture, hemp fibers exhibit a scale effect of tensile strength in that fiber strength increases with the reduction of gauge length [5]. The most prominent defects of hemp fibers are kink bands or dislocations that are local misalignments of cellulose microfibrils in the cell wall [8−10]. Kink bands can be observed, e.g., by polarized light microscopy as bright zones crossing most of or the entire fiber diameter and oriented roughly perpendicularly to fiber axis as seen in fig. 1.

Kink bands develop during growth [9] and processing [10] of hemp. A large scatter of strength and no correlation between the strength of hemp fibers with ca. 1 mm gauge length and the amount of kink bands present, characterized by their relative area, was reported in [8]. However, the relative amount of dislocations in this case was limited to about 0.2. Moreover, the effect of the

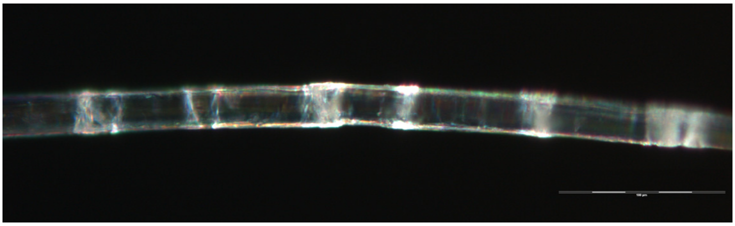

Figure 1: Elementary bast fiber of hemp with kink bands seen in transmitted polarized light as bright stripes (length of the scale bar is 100 μm).

dislocation amount on fiber strength may be relatively mild, as demonstrated in [18] for flax fibers, and thus could be overwhelmed by the scatter of strength.

In the present study, scale effect of the strength of elementary hemp fibers is explored experimentally, by tensile testing of fibers at two gauge lengths. Applicability of an analytical strength distribution function, derived assuming that kink bands control fiber fracture, to the description of hemp fiber strength is evaluated. Further, strength characteristics of the kink bands are derived from the fiber strength distribution.

2 Experimental

Hemp fibers were supplied by BaFa GmbH (Germany). As claimed by supplier, the average fiber length was 60 mm and content of shives (impurities) amounted to approximately 3%.

Single fiber tensile tests were performed according to the ASTM D 3379-75 standard [19]. Single filaments were manually separated from the fiber bundle. Two gauge length specimens were prepared with the free fiber length of 3 and 20 mm respectively. Fiber ends were glued onto a paper frame as shown in fig. 2.

Tensile tests of 20 mm long fibers were carried out on an electromechanical tensile machine Instron 4411 equipped with load cell of 5N and pneumatic grips. Experiments on 3 mm long filaments were carried out on a small Deben Microtest tensile stage equipped with 2N load cell and mechanical grips. During mounting the specimens were handled only by the paper frame. After clamping of the ends of the paper frame by the grips of the test machine, frame sides were carefully cut in the middle. The tests were displacement-controlled with the loading rate of 10%/min.

Diameter of every fiber was measured prior to the tensile test by using digital images obtained from optical microscopy. Olympus VANOX-T AH-2 microscope with DP-11 digital camera was used to take digital images along the fiber (three to five images per fiber, depending on its length). The images were stored on computer and analyzed later; up to five measurements were made from each image. All measurements for each fiber were pooled together and an average value of the diameter for every filament was calculated. These values were used to estimate the cross-section area of fiber (assuming circular shape of the fiber).

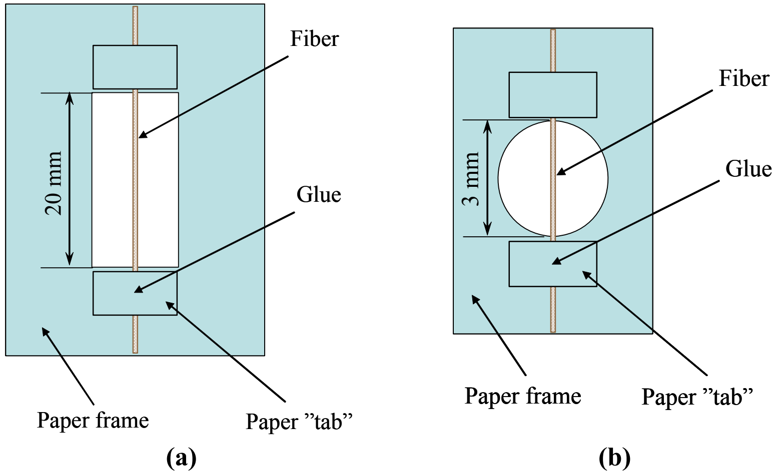

Figure 2: Schematic of single fiber tensile samples for (a) 20 mm and (b) 3 mm long filaments.

One should note that hemp fibers were rather uneven and sometimes twisted along their axis. Moreover, the shape of a fiber is not perfectly circular but rather elliptical. This of course introduced certain error in the estimation of fiber cross-section area. On the other hand, one can argue that the values were rather well averaged due to the number of measurements per fiber (15–25 measurements per sample). The presence of lumen in the fiber is not taken into account in calculation of cross-section area (the lumen size can reach up to several percent of the total cross-section area of a hemp fiber).

The fibers contained kink bands as shown in fig. 1. To quantify the linear density of kink bands in the fibers, a number of specimens of the type shown in fig. 2a but with 5 mm gauge length were prepared. The number of kink bands in each specimen was counted employing optical microscope with crossed polarizers.

3 Fiber strength distribution

Elementary hemp fibers may fail either at a macroscopic mechanical defect, such as kink bands, or at a microscopic flaw within the intact part of the fiber. If fiber failure at a kink band and due to failure in the intact part of the fiber may be considered as independent events, the probability of fiber failure is given by [20–21]:

$$P(\sigma) = 1 - \left(1 - P_k(\sigma)\right)\left(1 - P_i(\sigma)\right). \tag{1}$$

where the probability of fracture of a kink band in the fiber is designated as $P_k(\sigma)$, and fracture probability within the macroscopically intact part of the fiber is given by $P_i(\sigma)$.

The discrete macro-defect related fracture probability is expressed via the number of non-interacting defects n_k and defect strength distribution $P_d(\sigma)$ as follows [18, 22]:

$$P_k(\sigma) = 1 - \exp[-n_k P_d(\sigma)] . \qquad (2)$$

While the defect strength distribution can be treated as a characteristic of a given fiber batch, the number of defects may vary among fibers of the same length due to somewhat variable growth and processing conditions encountered by individual fibers. The linear defect density in a fiber of length l can be characterized by kink band spacing $s = l/n_k$. The random variability of s among fibers may be described by a two-parameter Weibull distribution

$$P_s(s) = 1 - \exp\left[-\left(\frac{s}{\bar{s}}\right)^m\right], \qquad (3)$$

where $\bar{s}$ is the Weibull scale parameter and m – the shape parameter. Assuming the Weibull two-parameter distribution for the defect strength:

$$P_d(\sigma) = 1 - \exp\left[-\left(\frac{\sigma}{\sigma_0}\right)^\rho\right], \qquad (4)$$

the low-strength tail of it has a power-law form $P_d(\sigma) \sim (\sigma/\sigma_0)^\rho$. Then, taking into account the random number of defects in eqn. (2), one arrives at the fiber strength given by the modified Weibull distribution [18, 20, 23]:

$$P_k(\sigma) = 1 - \exp\left[-\left(\frac{l}{l_0}\right)^\gamma \left(\frac{\sigma}{\beta}\right)^\alpha\right] \qquad (5)$$

where l_0 is a normalizing parameter with length dimension. The rest of distribution eqn. (5) parameters are related to those of kink band strength and spacing distributions as specified in [18, 20, 23]. The length exponent γ is found to depend only on the scatter of the kink band spacing among fibers, characterized by the shape parameter m of the distribution eqn. (3):

$$\gamma = m\big/\sqrt{m^2 + 1} . \qquad (6)$$

If the fiber strength distribution eqn. (5) and kink band spacing distribution eqn. (3) are known, kink band strength parameters can be evaluated by inverting the relations of [18] as follows:

$$\rho = \alpha\sqrt{m^2 + 1}\big/m \qquad (7)$$

$$\sigma_0 = \beta\left(\frac{l_0}{\bar{s}}\right)^{\frac{1}{\rho}} \Bigg/ \left[1-\rho^{-1.5}\left(m^2+1\right)^{-0.75}\right]. \tag{8}$$

Probability of failure in the intact part of the fiber, $P_i(\sigma)$, should be governed by the micro-defect distribution in the fiber, hence given by the Weibull distribution. It is also affected by the variability of fiber diameter, as discussed in [21, 24]. However, in the presence of macroscopic damage, failure at kink bands is likely to be the dominant fracture mechanism of bast fibers [21], thus eqn. (1) should reduce to the strength distribution given by eqn. (5).

4 Results and discussion

The average strength of elementary hemp fibers and the standard deviation of strength amounted to 239 (93) MPa for 20 mm fibers and 404 (268) MPa for 3 mm fibers. The strength values obtained are within the range reported in literature for different hemp varieties and fiber lengths and collected in table 1.

Counting the number of kink bands in fibers of 5 mm gauge length yielded the average spacing of 57 μm and standard deviation 11 μm. By the method of moments, the shape parameter of the spacing distribution eqn. (3) was evaluated at m = 6.6 and the scale parameter $\bar{s}$ = 0.061 mm. According to eqn. (6), the length exponent equals γ = 0.99. The remaining two parameters of the strength distribution eqn. (5) were determined as α = 2.80 and β = 738 MPa by fitting eqn. (5) to the strength data at 20 mm gauge length (and choosing l_0 = 1 mm). The empirical strength distribution for this gauge length is shown in fig. 3 together with the approximation by eqn. (5).

It follows from eqn. (5) that the average fiber strength depends on its length as

$$\langle\sigma\rangle = \beta\left(\frac{l}{l_0}\right)^{-\frac{\gamma}{\alpha}}\Gamma\left(1+\frac{1}{\alpha}\right) \tag{9}$$

where $\Gamma(x)$ is the gamma function. The experimental average strength data and the theoretical relation eqn. (9) are plotted in fig. 4. It is seen that eqn. (9), with the parameters determined form 20 mm fiber tests, provides accurate prediction of fiber strength at 3 mm gauge length thus corroborating the applicability of the strength distribution eqn. (5).

Employing eqns. (7) and (8), the Weibull distribution eqn. (4) parameters of kink band strength are evaluated as ρ = 2.83 and σ_0 = 2125 MPa. The relatively high value of the shape parameter of eqn. (3) signifies little variability in kink band content, as characterized by their spacing, among fibers. Consequently, strength scatter of the fibers is mainly due to variability of kink band strength, and the shape parameter values of eqns. (4) and (5) almost coincide. Furthermore, uniformity of the fibers in terms of damage content has also lead to the Weibull distribution of their strength, as a limiting case of the modified distribution eqn. (5) at the value of length exponent $\gamma \approx 1$.

Table 1: Strength of untreated elementary hemp fibers.

Gauge length l, mm	Particular features	Variety/supplier	Mean strength, MPa	Standard deviation, MPa	Ref.
~1	-	Felina/Danish Agricultural Research Center (Denmark)	1735	723	[8]
10	-	-/Hemptech NZ Ltd (New Zealand)	607	210	[5]
	taken from stem top	Fedora 17/Fibres Recherche Développement® (France)	394	214	[6]
	middle		482	337	
	bottom		368	275	
	-	-/LCDA (France)	285	-	[15]
	-	-/Hemcore (UK)	514	274	[16]
	-	-/AFT Plasturgie® (France)	788	307	[17]

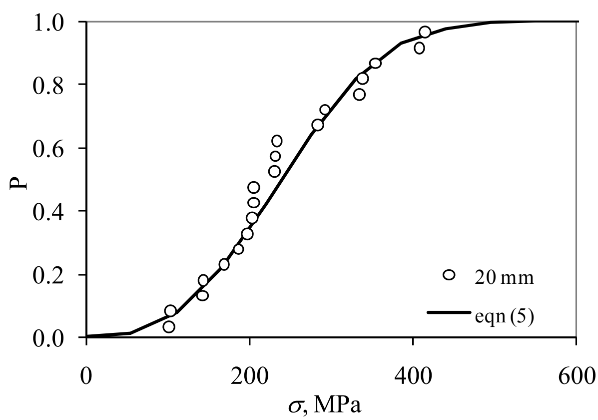

Figure 3: Strength distribution of elementary hemp fibers of 20 mm gauge length and its approximation by eqn. (5).

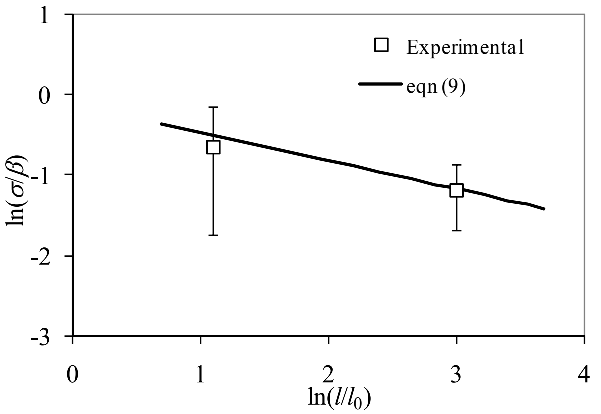

Figure 4: Average normalized strength of elementary hemp fibers as a function of fiber gauge length.

For comparison, kink band spacing and strength parameters, evaluated for elementary flax fibers by the procedure described above, are presented in table 2. One can see that the hemp fibers studied differ from those considered in [18, 20] in that their kink band strength is significantly lower at a rather high linear density, which results in a relatively low fiber strength. Since kink bands develop not only during growth but also in processing of the fibers, fiber strength can be increased by optimizing the latter.

Table 2: Kink band spacing, eqn. (3), and strength distribution, eqn. (4), parameters of elementary flax fibers.

Variety/supplier	m	$\bar{s}$, mm	ρ	σ_0, MPa	Ref.
ArcticFlax/FinFlax Oy (Finland)	1.40	0.21	3.6	2790	[20]
-/Ekotex (Poland)	5.16	0.067	3.2	3350	[20]
Elisa/Baltiks East SIA (Latvia)	3.74	0.069	2.18	5490	[18]

The model relating fiber damage to its tensile strength, proposed above, treats kink bands as uniform in terms of strength, characterized by the same strength distribution regardless of their size. Such a simplification appears appropriate only for a fiber batch obtained by the same (processing) procedure. Generally, the extent of kink bands and, possibly, their severity increase during processing [10, 25]. Therefore, the model should be extended to incorporate more detailed information on damage geometry and severity in fibers in order to enable more accurate description of bast fiber strength.

5 Conclusions

Tensile strength of elementary hemp fibers has been studied experimentally and the linear density of kink bands in fibers characterized by optical microscopy. Applicability of a strength distribution function accounting for the variability in defect content among fibers has been considered. The theoretical distribution was verified and found to provide acceptable accuracy in predicting the scale effect of strength. Strength characteristics of the kink bands have been evaluated by the model using the experimental fiber strength data.

Acknowledgements

J. Andersons gratefully acknowledges funding of his work by ERDF via project 2010/0290/2DP/2.1.1.1.0/10/APIA/VIAA/053.

R. Joffe would like to acknowledge that part of his work within this study has been supported by the Commission of the European Communities via funding granted to the Project "BIOCOMP", Proposal No. IP 515769-2.

The assistance of Dr. E. Spārniņš in characterization of kink bands by optical microscopy is acknowledged.

References

[1] Lilholt, H. & Lawther, J.M., Natural organic fibres. In: *Comprehensive Composite Materials*, vol. 1, ed. Kelly, A. & Zweben, C., Pergamon Press: New York, pp. 303-325, 2000.

[2] Hill, C. & Hughes, M., Natural fibre reinforced composites Opportunities and challenges. *Journal of Biobased Materials and Bioenergy*, **4**, pp. 148-158, 2010.

[3] Steger, J., Light Weight! No Matter What the Costs? Plant Fibres for Light Weight Automotive Applications. *Journal of Biobased Materials and Bioenergy*, **4**, pp. 181-184, 2010.

[4] Dissanayake, N.P.J., Summerscales, J., Grove, S.M. & Singh. M.M., Life cycle impact assessment of flax fibre for the reinforcement of composites. *Journal of Biobased Materials and Bioenergy*, **3**, pp. 245-248, 2009.

[5] Pickering, K.L., Beckermann, G.W., Alam, S.N. & Foreman, N.J., Optimising industrial hemp fibre for composites. *Composites: Part A*, **38**, pp. 461–468, 2007.

[6] Duval, A., Bourmaud, A., Augier, L. & Baley, C., Influence of the sampling area of the stem on the mechanical properties of hemp fibers. *Materials Letters*, **65**, pp. 797–800, 2011.

[7] Dai, D. & Fan, M., Characteristic and performance of elementary hemp fibre. *Materials Sciences and Applications*, **1**, pp. 336-342, 2010.

[8] Thygesen, L. G., Eder, M. & Burgert, I., Dislocations in single hemp fibres—investigations into the relationship of structural distortions and

tensile properties at the cell wall level. *Journal of Materials Science*, **42**, pp. 558–564, 2007.
[9] Thygesen, L. G. & Asgharipour, M. R., The effects of growth and storage conditions on dislocations in hemp fibres. *Journal of Materials Science*, **43**, pp. 3670–3673, 2008.
[10] Thygesen, L.G., The effects of growth conditions and of processing into yarn on dislocations in hemp fibres. *Journal of Materials Science*, **46**, 2135–2139, 2011.
[11] Fan, M., Characterization and performance of elementary hemp fibres: factors influencing tensile strength. *BioResources*, **5**, pp. 2307–2322, 2010.
[12] Mwaikambo, L.Y. & Ansell, M.P., Mechanical properties of alkali treated plant fibres and their potential as reinforcement materials. I. hemp fibres. *Journal of Materials Science*, **41**, pp. 2483–2496, 2006.
[13] Peetla, P., Schenzel, K.C. & Diepenbrock, W., Determination of mechanical strength properties of hemp fibers using near-infrared Fourier transform Raman microspectroscopy. *Applied Spectroscopy*, **60**, pp. 682–691, 2006.
[14] Korte, S. & Staiger, M.P., Effect of processing route on the composition and properties of hemp fibre. *Fibers and Polymers*, **9**, pp. 593-603, 2008.
[15] Placet, V., Characterization of the thermo-mechanical behaviour of Hemp fibres intended for the manufacturing of high performance composites. *Composites: Part A*, **40**, pp. 1111–1118, 2009.
[16] Beckermann, G.W. & Pickering K.L., Engineering and evaluation of hemp fibre reinforced polypropylene composites: Fibre treatment and matrix modification. *Composites: Part A*, **39**, pp. 979–988, 2008.
[17] Bourmaud, A. & Baley, C., Rigidity analysis of polypropylene/vegetal fibre composites after recycling. *Polymer Degradation and Stability*, **94**, pp. 297–305, 2009.
[18] Andersons, J., Spārniņš, E. & Poriķe, E., Strength and damage of elementary flax fibers extracted from tow and long line flax. *Journal of Composite Materials*, **43**, pp. 2653-2664, 2009.
[19] "Standard Test Method for Tensile Strength and Young's Modulus for High-Modulus Single Filament Material", ASTM D3379-75 (Reapproved 1989).
[20] Andersons, J., Poriķe, E. & Spārniņš, E., The effect of mechanical defects on the strength distribution of elementary flax fibers. *Composites Science and Technology*, pp. 2152–2157, 2009.
[21] Andersons, J., Poriķe, E. & Spārniņš, E., Modeling strength scatter of elementary flax fibers: the effect of mechanical damage and geometrical characteristics. *Composites Part A*, **42**, pp. 543–549, 2011.
[22] Todinov, M.T., Probability of fracture initiated by defects. *Materials Science and Engineering*, **A 276**, pp. 39–47, 2000.
[23] Curtin, W.A., Tensile strength of fiber-reinforced composites: III. Beyond the traditional Weibull model for fiber strengths. *Journal of Composite Materials*, **34**, pp. 1301-1332, 2000.

[24] Spārniņš, E. & Andersons, J., Diameter variability and strength distribution of elementary flax fibers. *Journal of Materials Science*, **44**, pp. 5697–5699, 2009.
[25] Aslan, M., Mehmood, S., Madsen, B. & Goutianos, S., The effect of processing on defects and tensile strength of single flax fibres. *Proc. of ECCM 14*, paper ID: 539-ECCM14, 2010.